Article

J. Mex. Chem. Soc. **2008**, *52(1)*, 67-73

ISSN 1870-249X

Bi and Three-Metallic Electrocatalysts Preparation for Methanol Oxidation

Yara Márquez-Navarro,* Laura Galicia,* Víctor Hugo Lara, and Gloria Del Ángel

Universidad Autónoma Metropolitana-Iztapalapa, Departamento de Química, San Rafael Atlixco 186 Col. Vicentina, Delegación Iztapalapa, Apdo. Postal 55-534, C. P. 09340, México D. F. (México) Tel. 58044671, Fax 58044666 iaruka@yahoo.com*, lgl@xanum.uam.mx*

Recibido el 26 de octubre de 2007; aceptado el 16 de febrero del 2008

Abstract. Bi and tri-metallic (Pt-Ru/C, Pt-Mo/C and Pt-Ru-Mo/C) catalysts were synthesized by using as precursors the metallic salts and applying the co-impregnation method. The tri-metallic catalysts underwent different thermal treatments and they were characterized by X-Ray. The catalytic activity for methanol oxidation reaction was determined by cyclic voltammetry (CV).
The results show that the materials calcined before reduction presented the highest catalytic activity for methanol oxidation reaction.
Key words: Electrochemical oxidation; methanol; Pt-Ru-Mo supported catalyst.

Resumen. Se sintetizaron catalizadores bi y tri-metálicos de (Pt-Ru/C, Pt-Mo/C and Pt-Ru-Mo/C) a partir de las sales precursoras empleando el método de co-impregnación. Los catalizadores tri-metálicos fueron sometidos a diferentes tratamientos térmicos, todos los materiales catalíticos fueron caracterizados por Rayos X. La actividad catalítica fue determinada mediante la reacción de oxidación de metanol aplicando la técnica de voltamperometría cíclica (CV).
Los resultados mostraron que los materiales calcinados antes de ser reducidos en flujo de H_2, presentaron una mayor actividad catalítica para la reacción de metanol.
Palabras clave: Electroxidación; metanol; catalizadores Pt-Ru-Mo soportados.

Introduction

Direct methanol fuel cells (DMFCs) have been studied for more than 30 years. These cells, which are based on the technology of proton exchange membrane fuel cells, are good candidates for various applications, mainly in electric vehicles and small devices such as mobile phones, laptops, and digital cameras [1]. However, under operational conditions, these systems exhibit low voltage efficiency due to the slow kinetics of the methanol oxidation, which means that the reaction occurs at high overpotentials [2-3].

Pt has been used as electrode for studying the methanol oxidation reaction. Since, the oxidation of methanol, on a Pt electrode is followed by the formation of intermediates, like CO, which are strongly adsorbed on the catalyst surface, reducing considerably its electroactivity [4]; it is necessary therefore to have catalysts whose surface be resistant to the CO poisoning species [5].

The Pt-Ru bimetallic catalyst is commonly accepted as the best electrocatalyst for methanol oxidation. Ru provides oxygenated species at low potential in the vicinity of Pt sites, creating additional active sites for CO_{ads} oxidation [6]. Attempts have been made to improve the CO tolerance of Pt-Ru by the addition of a third metal such as Mo obtaining good catalysts to achieve the satisfactory oxidation of methanol [6-9].

Electro-oxidation of CO on supported Pt-Ru-Mo [7] is higher performing than the Pt-Ru catalyst. Indeed, the mixing of Pt with Mo leads to weakly adsorbed CO on Pt sites and OH strongly adsorbed only on Mo sites [8]. Such tri-metallic catalysts favor the formation of OH_{ads} species, which assist in the oxidation of CO_{ads}. Several synthetic routes have been reported for the preparation of catalysts from transition metals, including the alloys formation, electrodepositions, co-depositions, by adsorption or using sol-gel systems [10-16].

Simple preparation method used in heterogeneous catalysis such as co-impregnation is known for obtaining small particles. This synthesis method have several advantages: the precursor salt does not produce impurities, nanometer-sized particles are obtained, and these particles turn out to be well dispersed over the support [17]. Furthermore, it is possible to tailor the catalyst controlling the particle size.

The purpose of this work is to prepare Pt-Ru/C, Pt-Mo/C and Pt-Ru-Mo/C catalysts with nanometric particle size by using simple co-impregnation method. It has been studied the calcination effects prior reduction on the metal particle size and the electrocatalytic activity for the methanol electro-oxidation.

Experimental

1. Chemicals

The precursor salts used in this work were H_2PtCl_6 (99.9% STREM CHEMICALS), $RuCl_3$ (99% STREM CHEMICALS), and $Mo(CO)_6$ (98% STREM CHEMICALS), and the support was graphite powder (99.9% ALFA AESAR A JOHNSON MATHEY) with a 140 m^2g^{-1} surface area [18].

2. Catalysts preparation

2.1 Co-impregnation method

To obtain the Pt-Ru and Pt-Mo catalysts by the co-impregnation method, we added the precursor salts H_2PtCl_6, $RuCl_3$ and $Mo(CO)_6$ in a 1:1 atomic ratio dissolved in ethanol, to the graphite support. These mixtures were maintained under constant mechanical stirring for 12 hours, to obtain a homoge-

neous mixture. The solvent in excess was then eliminated by heating at 70°C for 15 hours. Finally, the powders containing the precursor salts were subjected to a thermal reduction treatment at 300°C for 3 hours under a hydrogen flow (H_2 INFRA, chromatographic grade 99.99%) at a 60 ml/min rate.

The tri-metallic Pt-Ru-Mo were prepared by impregnation of Pt-Ru/C catalyst with a precursor salt $Mo(CO)_6$ to obtain with 2 wt % respect to the catalyst. Three tri-metallic catalysts underwent the following thermal trealments: one was directly reduced on hydrogen at 300°C for 3 hours (CoIM/C); the other two ones were first oxidized in air at 300°C and 500°C (CoIM3/C and CoIM5/C) respectively before the reduction for 3 hours under H_2 flow at 300°C was performed.

3. Physical characterization

3.1 X-ray diffraction

In a Siemens diffractometer with Cu Ká radiation (1.54 Å wavelength) operated at 35 keV and 25 mA, X-ray diffraction (XRD) patterns were obtained at a 2° min^{-1} rate for values of 2θ between 30° and 60°. The species were identified by matching with the database of JCPDS cards [19]. The crystal size distribution of the tri-metallic catalysts was obtained from the right or left profile of the corresponding diffraction peak measured using the program XTLSIZE. In order to obtain the particle size distribution it is use the Scherrer equation:

$$dP = \frac{\kappa\lambda}{(B\cos\theta)}$$

The parameters used to obtain the particle distribution are: the wavelength (λ), the diffraction angle (θ), the peak broad (B) and the Scherrer constant (κ).

4. Electrochemical study

To determine the influence of the catalysts synthetic method on the methanol oxidation, an electrochemical study was performed using Cyclic Voltammetry (CV). The voltammetric responses were obtained using a BAS 100B; Bioanalytical Systems potentiostat, which was coupled to a PC and equipped with a conventional three-electrode cell with a jacket for temperature control; the three electrodes used were a graphite bar as the counter electrode, a mercury|mercurous sulfate electrode in saturated K_2SO_4 (SSE) was used as the reference electrode, all the potential in this work are referred to it; and the synthesized catalyst as the working electrode. The electrochemical experiments were carried out at room temperature under a nitrogen atmosphere, using a 20mV/s scan rate over the potential interval -500 to 500 mV *vs* SSE. The supporting electrolyte for all the experiments was 0.5 M H_2SO_4 + 2M CH_3OH. All solutions were prepared with deionized water and the reagents were of analytic grade.

The three-metallic catalysts properties were electrochemically studied in acidic medium methanol oxidation reaction. In this work it has been used a 0.5 M H_2SO_4 + 2M CH_3OH solution. In order to select an adequate methanol concentration for this study, it has been done a previous study at different methanol concentrations, and it has been found that 2M methanol concentration was the optimum one. The results are not reported in this work.

4.1 Preparation of the working electrode

The working electrode was prepared by mixing the bi or tri-metallic catalyst with mineral oil (Nujol) as agglomerate in a 1:1 ratio by weight. This paste was packed in a plastic tube with a geometric surface area of 0.07068 cm^2. The electric connection was made by copper wire.

Results and Discussion

X-ray diffraction characterization

In Fig. 1a. and 1b. there are shown the difractogram for the bi-metallic Pt-Ru and Pt-Mo catalyst respectively. In the difractogram 1a., there are shown the signals corresponding to the Pt/C (111) and (200) crystallographic planes at a 2θ = 40.11° and 46.47° respectively, and for Ru/C the (101) crystallographic plane it is shown at 2θ = 44.55°. For the 1b. difractogram, the Pt crystallographic planes were shown at 2θ = 39.96° and 46.26°, and the main characteristic of this signal is the asymmetry due to the presence of a shoulder around 2θ = 40.53; which has been decoupled by a deconvolution to this signal, and it could be detected that the asymmetry was due to a Mo signal which corresponds to Mo (100) according a the JCPDS card.

The diffractogramms corresponding to the bimetallic catalyst were compared with respect to the monometallic ones. The signals corresponding to Pt/C are presented at 2θ = 39.763 (111) and 2θ = 46.243 (200), and for Ru/C at 2θ = 38.385 (101), 2θ = 44.00 and Mo/C at 2θ = 40.509 (110) and 2θ = 58.599 (200), the values are in agreement with respect to the JCPDS cards.

By analyzing the diffractograms one can observe that the signals associated to the Pt(111) in the Pt-Ru/C catalyst are presented at 2θ values higher than in the case of the Pt-Mo/C catalyst. This behavior can be attributed to a strong interaction among the Pt-Ru/C metal particles [20]. For the case of the Pt-Mo/C catalyst the Pt (111) and (200) signals are shown at the values reported in the literature [21]. It can be concluded that the Mo does not form any alloy.

For the case of the tri-metallic catalyst, it is shown only the diffractogram for the CoIM3 tri-metallic catalyst (Fig 2), due that in all cases it was obtained a similar pattern. These catalysts exhibit diffraction peaks corresponding to Pt (111) at 2θ = 39.86° and (200) at 2θ = 46.36, for to Ru (101) at 2θ = 43.86° and Mo (100) at 2θ = 40.30° according to JCPDS cards. In Table 1, it is shown the values for the signals obtained from the X-ray diffraction patterns for the bi and tri-metallic catalysts.

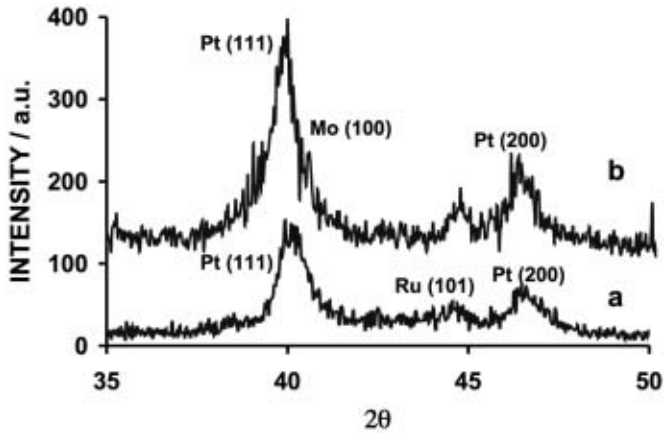

Fig. 1. XRD Patterns of a) Pt-Ru/C and b) Pt-Mo/C catalysts supported on graphite synthesized for co-impregnation.

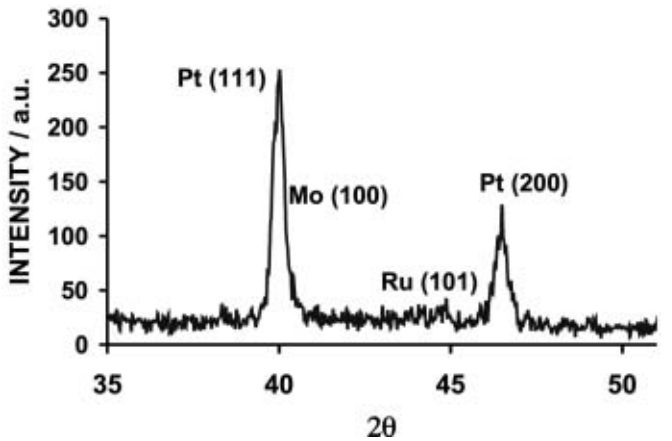

Fig. 2. XRD Patterns of Pt-Ru-Mo catalysts supported on graphite synthesized by co-impregnation (CoIM3/C).

Table 1. Results obtained for the catalysts X-ray studies.

Catalyst	Metal	Crystallographic plane	2θ
Pt-Ru/C	Pt	(111), (200)	40.11º, 46.47º
	Ru	(101)	44.55º
Pt-Mo/C	Pt	(111), (200)	39.96º, 46.26º
	Mo	(100)	40.56º
CoIM/C	Pt	(111), (200)	40.14º, 46.65
	Ru	(101)	41.94º
	Mo	(100)	40.24º
CoIM3/C	Pt	(111), (200)	39.86º,46.36º
	Ru	(101)	43.86º
	Mo	(100)	40.30º
CoIM5/C	Pt	(111), (200)	39.89º, 46.39º
	Ru	(101)	43.97º
	Mo	(100)	40.54º

Table 2 Relative intensity of the molybdenum or ruthenium peak to the Pt (111) peak

Catalysts	Relative intensity (%)	$I_{Mo(110)}/I_{Pt(111)}$	$I_{Ru(101)}/I_{Pt(111)}$
Pt-Ru/C			
Pt (111)	54.55		
Pt (200)	26.14		0.35
Ru (101)	19.32		
Pt-Mo/C			
Pt (111)	54.45		
Pt (200)	21.78	0.43	
Mo (100)	23.76		
Co-impregnation and reduction (CoIM/C).			
Pt (111)	46.16		
Pt (200)	21.96	0.56	0.12
Ru (101)	5.85		
Mo (100)	26.03		
Oxidation, reduction, and co-impregnation 300°C (CoIM3/C).			
Pt (111)	66.19		
Pt (200)	27.74	0.05	0.04
Ru (101)	2.73		
Mo (100)	3.35		
Oxidation, reduction and co-impregnation 500°C (CoIM5/C).			
Pt (111)	68.60		
Pt (200)	23.81	0.04	0.06
Ru (101)	4.63		
Mo (100)	2.96		

From the X-ray diffraction patterns of the tri-metallic catalysts, we estimated the relative intensity of each metal through the reflections of Pt (111), Pt (200), Ru (101) and Mo (100) (Table 2) assuming that the X-ray absorption is similar and, therefore, that the percentage is proportional to the X-ray diffraction peak areas. Also, in Table 2 the relative metallic intensities for the bimetallic catalyst are reported. For the bimetallic catalyst, Pt signal intensity is higher than the Ru and Mo ones, even though the atomic relation is 1:1.

For the tri-metallic catalysts it is observed an interesting behavior. The $I_{Mo(100)}/I_{Pt(111)}$ ratios in CoIM/C with respect to the once in the CoIM3/C and CoIM5/C catalyst shows that, molybdenum is segregated on the catalytic surface. This segregation is diminished in the CoIM3/C and CoIM5/C where almost all molybdenum is undetected independently of the thermal treatment. However, if the catalyst is oxidized and then reduced, the Ru peak almost fades out showing again that ruthenium is highly dispersed forming very small particles on the support.

The X-ray provides the crystallite size distribution from each peak profile; therefore the distribution corresponding to each metal.

In Pt-Ru/C and Pt-Mo/C catalysts (Fig. 3a and 3b); the crystallite size distribution corresponds to the same diameter interval for Pt (1 to 14nm). Thus, the preparation method leads to the formation of Pt crystallites with similar size.

Instead, ruthenium crystallite size distribution is comprised between 1 and 8 nm, and molybdenum distribution is comprised between 1 and 7 nm, it is also observed the formation of particles with greater size but in quite small proportion.

In the case of the catalyst CoIM/C (Fig. 4), the Pt crystallites exhibit a wider size distribution (1-22 nm), the biggest amount is located between 6-19 nm, while the Ru and Mo crystallite distributions are comprised between 1 and 10 nm.

Figure 5a shows the diameter distribution profile of the Pt, Ru and Mo crystallites for catalyst CoIM3/C. This profile shows that the co-impregnation synthesis method, combined with the thermal treatment used for this catalyst, gives rise to metallic particles with multimodal distributions for all the metals, Pt, Ru and Mo. For Pt, for example, almost all particles have sizes in the small interval of 19-29 nm; although a small peak is observed in the interval 7-11 nm, it represents a negligible percentage. The Pt particle sizes for CoIM3/C are larger than for CoIM/C. These means that on a graphite support the mobility of the Pt oxidized species leads to a sinterization of the Pt at 300 °C, which explains the formation of larger Pt particles in these catalysts.[22]

The Ru particles on CoIM3/C exhibit a diameter distribution that is slightly wider and clearly asymmetric in the interval of 1-15 nm. However, the width of this distribution is bigger than the ones observed for the CoIM/C catalyst. On the other hand, the diameter distribution for Mo in CoIM3/C is similar to that of Pt, spanning the interval 18-27 nm.

For the catalyst CoIM5/C, the particle diameter distribution (Fig. 5b) is similar to that obtained for CoIM3/C, although, the distributions of Pt, Ru and Mo, are different. In general slightly larger crystals are present on the surface of CoIM5/C than on the CoIM3/C one. For example, the Pt distribution is multi-modal in the interval 16-29 nm, and the Ru and Mo particles exhibit diameter distributions over intervals of 1-21 nm and 1-9 nm respectively.

The characterization of the catalysts in the X-ray diffraction studies showed that the catalysts exhibited different particle sizes and distributions for those particles over the graphite. Hence, the synthesis method determines the particle size, shape and distribution on the graphite surface.

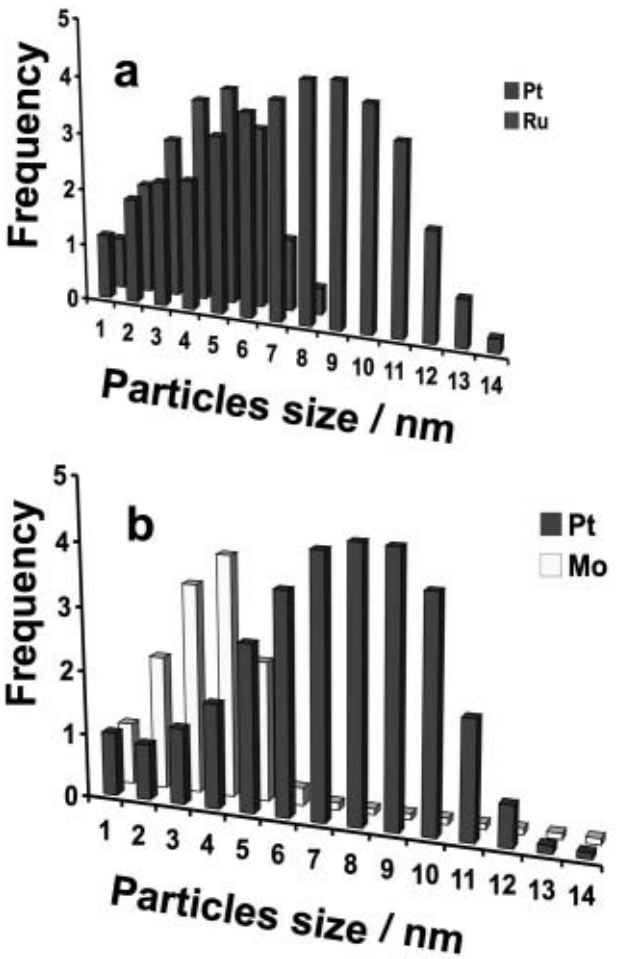

Fig. 3. Distribution profile of the particle diameters obtained by X-ray diffraction for bi-metallic catalysts: a) Pt-Ru/C y b) Pt-Mo/C.

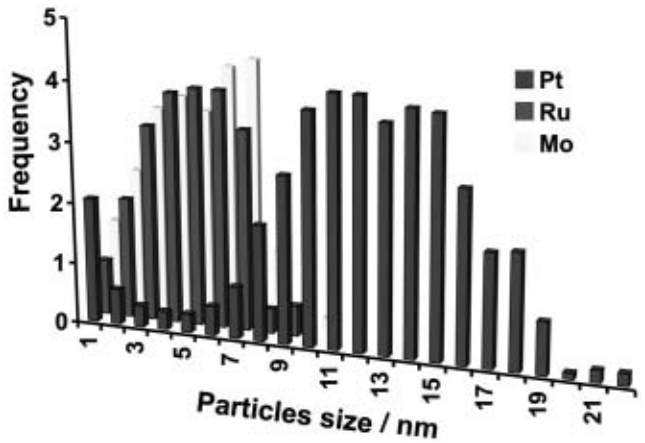

Fig. 4. Distribution profile of the particle diameters obtained by X-ray diffraction for tri-metallic catalysts CoIM/C.

Oxidation of methanol on the Pt-Ru/C and Pt-Mo/C catalysts

Figure 6a and 6b show the voltamperograms of methanol oxidation with Pt-Ru/C and Pt-Mo/C. In both voltammograms there are observed the direct oxidation peaks (A) and a methanol reoxidation peak (B). The current intensity and the oxidation potential peaks obtained are different for the two bimetallic catalysts. The big increase in the oxidation current in Pt-Ru/C (84.9 μAcm^{-2}), may be attributed to a higher amount of Pt on the surface (Table 2). In the case of the Pt-Mo/C, the

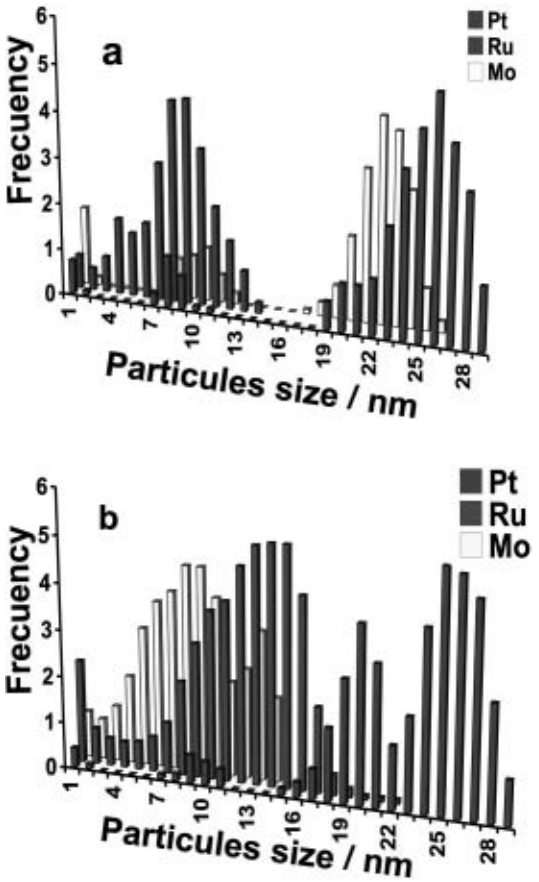

Fig. 5. Distribution profile of the particle diameters obtained by X-ray diffraction for tri-metallic catalysts: a) CoIM3/C and b) CoIM5/C.

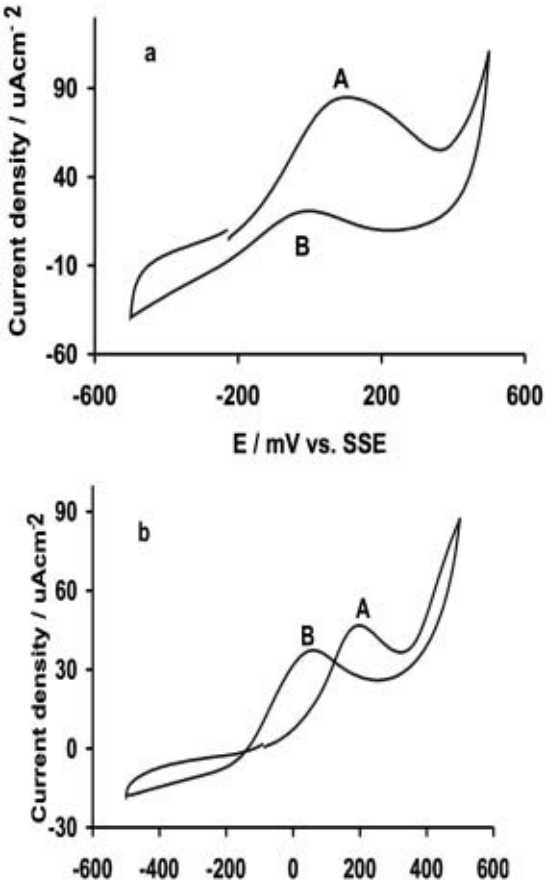

Fig. 6. Oxidation of methanol in a supporting electrolytic of 0.5 M H_2SO_4 + 2 M CH_3OH, at a scan rate of 20 mVs^{-1}: a) Pt-Ru/C and b) Pt-Mo/C.

oxidation current obtained is lesser (46.8 μAcm^{-2}), which can be related to less amount of Pt on the surface, because the Mo is deposited on the Pt. This Mo behavior has been previously reported [21].

Another feature of those catalysts is the variable broadening of the methanol oxidation peaks. The Pt-Ru/C catalyst present a broader peak than Pt-Mo/C, hence in Pt-Ru/C the oxidation reaction follows a mechanism with intermediary compounds formation and it is a not very selective reaction; this conclusion is verified when the scanning direction is inverted since a lower intensity signal appears at lower positive potentials, this signal is attributed to methanol re-oxidation.

For the Pt-Ru/C catalyst the re-oxidation current contribute with 24.5%; whereas the Pt-Mo/C catalyst the re-oxidation current contributes with 79.7% (Table 3). This feature is attributed to the high tolerance of the Pt-Mo/C [23].

As it has been reported, Mo sites adsorb oxygen-hydroxide species that act as CO oxidation reagents. In this case it can be assumed the small Mo particles are dispersed on the Pt particles surface. As a consequence, the oxygen species adsorbed on Mo are near to CO adsorbed on Pt favoring the oxidation to CO_2. Therefore the Mo leads to an enhanced catalytic activity, diminishing the formation of intermediated compounds.

The Pt-Ru/C catalysts show a high current (84.9 μAcm^{-2}) and a low oxidation potential for methanol (108 mV) than the Pt-Mo/C (202 mV). Because of the dissociate methanol character its decomposition requires an ensemble of the Pt atoms, leading to a possible geometric effect [24]. The presence of Ru in Pt-Ru/C catalyst promotes a weakening of Pt-CO bond producing easily the CO oxidation reaction to CO_2.

As it has been showed above the particles size distribution for Pt, Ru and Mo are very similar for both catalysts then we can think that a possible different distribution of Ru and Mo on the Pt surface could occurred and be responsible of the differences observed on both catalysts. By other hand, it is broadly known that the addition of the Ru and Mo to Pt enhances CO removal from the surface. Since Ru and Mo promotes CO oxidation to CO_2 via a bifunctional mechanism [25-27].

Hence, the combination of the properties of these catalysts is a good option for tri-metallic catalysts with a methanol efficiency performance.

Table 3. Currents and potentials for the oxidation and re-oxidation of methanol for the catalysts.

Catalysts	E_{direct} (mV) vs. SSE	j_{direct} (μAcm^{-2})	$E_{inverse}$ (mV) vs. ESS	$j_{inverse}$ (μAcm^{-2})	$j_{inverse}/j_{direct}$x100%
Pt-Ru/C	108	84.9	4	20.8	24.50
Pt-Mo/C	202	46.8	54	37.3	79.70
CoIM/C	208	61.75	57	26.42	44.43
CoIM3/C	180	442.45	40	212.63	48.06
CoIM5/C	184	337.40	18	196.39	58.21

Oxidation of methanol on tri-metallic CoIM/C, CoIM3/C and CoIM5/C catalysts

Figs. 7 (a, b and c) displayed the voltammograms obtained for the electro-oxidation of methanol on the tri-metallic catalysts CoIM/C, CoIM3/C and CoIM5/C respectively. This voltammograms show the same electrochemical behavior to that obtained for the bi-metallic case, a direct methanol oxidation peak and the re-oxidation peak; nevertheless, the obtained currents for the methanol oxidation reaction are different among the tri-metallic catalysts. For example the non calcined sample (CoIM/C) catalyst (Fig. 7a) shows lower current than the ones obtained for the thermally treated tri-metallic catalysts (Figs. 7b and 7c). This fact can be associated to smaller Pt particles present on the CoIM/C surface, which favors the surface poisoning by CO as it has been reported [28].

An effect of the thermal treatment on the electrochemical properties (oxidation current) is observed. Fig. 7a shows lower current (61.75 μAcm^{-2}), CoIM3/C (442.45 μAcm^{-2}), CoIM5/C (337.4 μAcm^{-2}), Figs. 7b and 7c. This fact could be related to the difference of the Pt distribution particles size. For the CoIM/C catalyst the distribution is around 7-19 nm, similar to the values of bimetallic catalysts. Whereas the calcined samples (CoIM3/C, CoIM5/C) show larger particles sizes around 19-29 nm.

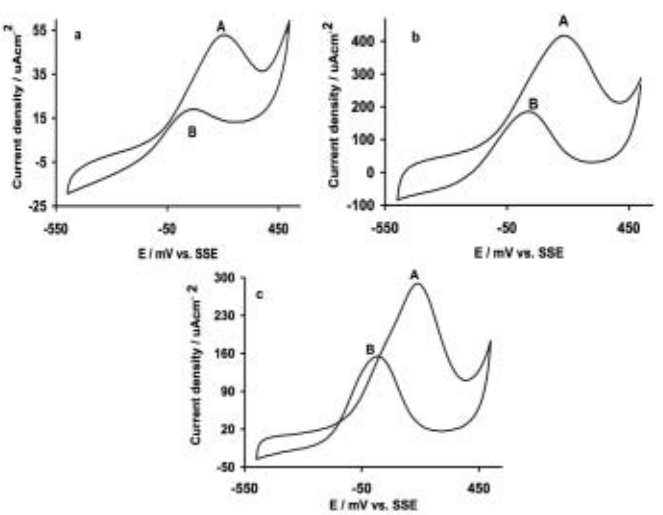

Fig. 7. Oxidation of methanol in a supporting electrolytic of 0.5 M H_2SO_4 + 2 M CH_3OH, at a scan rate of 20 mVs^{-1}: a) CoIM/C, b) CoIM3/C and c) CoIM5/C.

However, the voltammograms for CoIM3/C and CoIM5/C (Fig 9b and 9c) show the peak (A), corresponding to the oxidation of methanol, which are less anodic overpotentials than the ones was observed for CoIM/C. In addition, peak A, in the CoIM3/C and CoIM5/C voltammograms, is better defined than in the case of the voltammograms for CoIM/C. This result indicates that the oxidation of methanol to CO_2 is performed in more selective way on the calcined catalysts than on the non calcined one.

However CoIM5/C present the best selectivity to CO_2 for the methanol oxidation than CoIM/C and CoIM3/C, this result could be associated to small Mo particles deposited on large Pt surface additionally to the presence or Ru on the surface of Pt. The precalcination in air prior to reduction results in an increment in the surface of Ru concentration [22, 29]. The presence of the Ru and Mo on the surface of Pt summarizes the beneficial bifuncional effects. The optimum size distribution of the metal particles seams to be the one showed by the CoIM5, increasing the catalytic activity and tolerance to CO poisoning.

On reversing the potential at the switching potential ($E_{+\lambda}$) and scanning in the cathodic direction, a peak (B) is observed for all the catalysts. The diminution in the current (peak B), corresponding to the oxidation of methanol when the scan is reversed, can be attributed to the formation of RuO_2 which is formed during the thermal treatment or in parallel with the process of methanol oxidation to CO_2 during the forward scan [29]. These metallic oxides remain strongly adsorbed to the electrode surface, and thus reduce the availability of the metal surface for the re-oxidation of methanol during the reverse scan.

Table 3 summarizes the results obtained for the oxidation of methanol on the catalysts. This table lists the oxidation potentials for the direct conversion of methanol to CO_2, as well as the potentials obtained when the scan is switched towards cathodic potentials and the corresponding current intensities.

As shown in the Table 3, the catalysts calcined before reduction exhibit a higher oxidation current density at lower overpotentials. These results imply a possible diminishment on the poisoning by CO of the Pt metal surface of the working electrode. However, the value of $J_{inverse}/J_{direct}$ is higher in CoIM5/C catalyst (Table 3). The different behavior between the CoIM3/C, CoIM5/C catalysts could be related to the size and structure of the bimetallic catalysts.

As it was mention above, small particles favors probably a strong interaction on Pt, which promotes a Pt-CO bond weak-

ening on CoIM5/C catalysts leading to easily CO oxidation to CO_2. The tri-metallic catalyst CoIM5 calcined to 500 °C and reduced at 300 °C showed the best tolerance to CO poisoning this property is associated to the small Mo particles.

Conclusions

The co-impregnation method was applied in the synthesis of bi and tri-metallic catalyst (Pt, Ru and Mo) supported on graphite. The catalyst that did not undergo calcinations (CoIM/C), showed smaller Pt particle size than the calcined ones (CoIM3/C and CoIM5/C). The presence of small Mo and Ru particles on the Pt surface in CoIM5/C favors a higher tolerance to CO poisoning. CoIM3/C and CoIM5/C were characterized by a great amount of Pt present on the surface which formed different size particles. The former result is evidence that the bifunctional mechanism is privileged.

Therefore the impregnation method followed by a pre-calcination at 500 °C prior to the catalyst reduction produces a Pt-Ru-Mo/C catalyst with higher tolerance to CO poisoning during the methanol electroxidation.

Acknowledgements

Y. Márquez gratefully acknowledges the scholarship from CONACyT to pursue her postgraduate studies and LG wish to thank the CONACyT for financial support at the project no. 2115-35135.

References

1. Ren, X.; Zelenay, P.; Thomas, S.; Davey, J.; Gottesfeld S. *J. Power Sources.* **2000,** *86*, 111-116
2. Maillard, F.; Bennefont, A.; Chatenet, M.; Guétaz, L.; Doisneau-Cottignies, B.; Roussel, H.; Stimming, U. *Electrochimica Acta* **2007,** *53*, 811-822
3. Tong, Y.Y.; Kim, H.S.; Babu, P. K.; Waszczuk, P.; Wieckowski, A.; Oldfield, E. *J. Am. Chem. Soc.* **2002,** *124*, 468-473
4. Iwasita, T. *Electrochimica Acta.* **2002**, *47*, 3663-3674
5. Oliveira Neto, A.; Pérez, J.; Napporn, W. T.; Ticianelli, E. A.; González E. R. Workshop *Electrocatalysis in Indirect and Direct Methanol PEM Fuel Cell*, 3rd International Symposium in Electrocatalysis. Portoroz, Slovenia, **1999**, 83
6. Lima, A.; Coutanceau, C.; Léger, J.-M.; Lamy, C. *J. Appl. Electrochem.* **2001,** *31*, 379-386
7. Papageorgopoulos, D. C.; Keijzer, M.; Bruijn, F. A. *Electrochimica Acta* **2002,** *48*, 197-204
8. Shubina, T. E.; Koper, M. T. M. *Electrochimica Acta.* **2002**, *47*, 3621-3628
9. Gota, M.; Wendt, H. *Electrochimica Acta.* **1998,** *43*, 3637-3644
10. Guo, J. W.; Zhao, T. S.; Prabhuram, J.; Chen, R.; Wong C. W. *Electrochimica Acta* **2005**, *51*, 754-763
11. Santiago, E. I.; Camara, G. A.; Ticianelli, E. A. *Electrochimica Acta* **2003,** *48*, 3527-3534
12 Jeng, K. T.; Chien, C. C.; Hsu, N. Y.; Yen, S. C.; Chiou, S.-D.; Lin, S. H.; Huang, W. M. *J. Power Sources* **2006,** *160*, 97-104
13. Shao, Z.G.; Zhu, F.; Lin, W. F.; Christensen, P. A.; Zhang, H.; Yi, B. *J. Electrochem. Soc*. **2006,** 153, A1575-A1583
14. Arico, A. S.; Baglio, V.; Di Blasi, A.; Modica, E.; Antonucci, P. L.; Antonucci V. *J. Electroanal. Chem*. **2003,** *557*, 167-176
15. Arico, A. S.; Baglio, V.; Di Blasi, A.; Modica, E.; Monforte, G.; Antonucci, V. *J. Electroanal. Chem.* **2005,** *576*, 161-169
16. Mao, Q.; Sun, G.; Wang, S.; Sun, H.; Wang, G.; Gao, Y.; Ye, A.; Tin, Y.; Xiu, Q. *Electrochimica Acta* **2007,** *52*, 6763-6770
17. Burstein, G. T.; Barnett, C. J.; Kucernak, A. R.; Williams, K. R. *Catalysis Today.* **1997,** *38***,** 425-437
18. He, C.; Kunz, H. R.; Fenton, J. M. *J. Electrochem. Soc.* **1997**, *144*, 970-979
19. Azaroff, L. V. *Elements of X-ray Crystallography*, McGraw-Hill, New York, **1968**
20. Park, K.-W.; Choi, J.-H.; Lee, S.-A.; Pak, C.; Chang, H.; Sung, Y.-E. *J. of Catalysis.* **2004,** *224*, 236-242
21. Mukerjee, S.; Urian, R. C. *Electrochimica Acta* **2002,** *47*, 3219-3231
22. Alerasool, S.; Boecker, D.; Rejai, B.; González, R.; Del ángel, G.; Asomoza, M.; Gómez R. *Langmuir*, **1988**, 4, 1083-1090
23. Mukerjee, S.; Lee, S. J.; Ticianelli, E. A.; McBreen, J.; Grgur, B. N.; Markovic, N. M.; Ross, Jr. P. N.; Giallombardo, J. R.; De Castro, E. S. *Electrochem. Solid-State Letters.* **1999,** 2 (1), 12-15
24. Gasteinger, H. A.; Markovic, N.; Ross, Jr. P. N.; Cairns, E. *Electrochimica Acta* **1994**, *39*, 1825-1832
25. Hammett, A. Mechanism of Methanol Electro-oxidationin "*Intefacial Electrochemistry: Theory, Experiment, and Applications*" (Wieckowski A., Ed.) p. 843, Dekker, New York, **1999**
26. Watanabe, M.; Motoo, S. *J. Electroanal. Chem*., **1975**, *60*, 275-283
27. Gasteinger, H. A.; Markovic, N.; Ross, Jr. P. N.; Cairns, E. *J. Phys. Chem*. **1993**, *97*, 12020-12029
28. Santiago, E. I.; Batista, S. M.; Assaf, E. M. *J. Electrochem. Soc.* **2004,** 151, 7, A944-A949
29. Ordóñez, L. C.; Roquero, P.; Sebastian P. J.; Ramírez, J. *Catalysis Today*. **2005,** *107*, 46-52